

Monte Carlo track structure for radiation biology and space applications

H. Nikjoo¹, S. Uehara², I.G. Khvostunov³, F.A. Cucinotta⁴, W.E. Wilson⁵, D.T. Goodhead¹

1. MRC Radiation and Genome Stability Unit, Harwell, OX11 0RD (UK)
2. School of Health Sciences, Kyushu University, Fukuoka (Japan)
3. MRRRC, Medical Radiological Research Centre, Obninsk (Russia)
4. NASA, Johnson Space Center, Houston Texas 77058 (USA)
5. Washington State University, Richland, WA 99352 (USA)

Abstract

Over the past two decades event by event Monte Carlo track structure codes have increasingly been used for biophysical modelling and radiotherapy. Advent of these codes has helped to shed light on many aspects of microdosimetry and mechanism of damage by ionising radiation in the cell. These codes have continuously been modified to include new improved cross sections and computational techniques. This paper provides a summary of input data for ionizations, excitations and elastic scattering cross sections for event by event Monte Carlo track structure simulations for electrons and ions in the form of parametric equations, which makes it easy to reproduce the data. Stopping power and radial distribution of dose are presented for ions and compared with experimental data. A model is described for simulation of full slowing down of proton tracks in water in the range 1 keV to 1 MeV. Modelling and calculations are presented for the response of a TEPC proportional counter irradiated with 5 MeV alpha-particles. Distributions are presented for the wall and wall-less counters. Data shows contribution of indirect effects to the lineal energy distribution for the wall counters responses even at such a low ion energy.

KEYWORDS: Monte Carlo, Cross-Sections, Microdosimetry, TEPC.

1. Introduction

There are a number of codes describing transport and simulation of radiation tracks in biological environment. These codes could be classified as those providing information at macroscopic level, known as *condensed history* (CH) codes, used for example, in radiation therapy and industrial applications (Table I) and a second group describing tracks, interaction by interaction at the molecular level in DNA and cell. Table II shows a partial listing of the Monte Carlo track structure codes (MCTS) reported in the literature and widely used for modelling effects of ionising radiation. In the CH codes the transport of particle has been made by grouping together a large number of individual collisions using multiple scattering theory to calcu-

late the energy loss and the scattering angle. CH codes have been very successful in simulation of the transport of electrons and photons for absolute dose calculations in radiotherapy and estimation of relative dose in many dosimeters.

Development of event by event Monte Carlo track structure codes has been rather slower than the CH codes as the former require specification of all individual types of interaction cross sections for a particular medium under test (such as water vapour, liquid water and DNA). The codes listed in Table II cover the energy range 1 eV to 10 MeV for electrons and greater than 0.3 MeV/u for ions. Some codes also have extension for simulation of the ensuing chemistry following hydrolysis of water, generating distribution of stable radical species at a pico second. All codes use the same data-base of

Table I – Monte Carlo Track Codes in Radiation Research.

Code	Author	Medium	Particle	Energy Range	ref
ETRAN	Berger & Seltzer	all	e ⁻ & phot	10 keV - 1 GeV	[1]
EGS4	Nelson	all	e ⁻ & phot	10 keV - 1 GeV	[2]
PTRAN	Berger	H ₂ O	proton	50 - 250 MeV	[3]
MCNP	Briemeister	all	neutron	eV – MeV	[4]
PENELOPE	Salvat	all	e ⁻ & e ⁺	1keV-100MeV	[5]
PREGRINE	Hartmann Siantar	tissue	phot. & e ⁻	Therapy beam	[6]

Table II – Monte Carlo Track Codes in Radiation Biology.

Code	Author	Medium	Particle	Energy Range	Ref
<i>ATRACK</i>	Katz <i>et al</i>	all	e ⁻ & ions	up to GeV	[7]
<i>MOCA8</i>	Paretzke	H ₂ O (v, l)	e ⁻	10 eV – 100 keV	[8]
<i>OREC</i>	Turner <i>et al</i>	H ₂ O (l)	e ⁻	10 eV – 1 MeV	[9]
			p & a	0.3 – 4 MeV/u	
<i>STBRGEN</i>	Chatterjee & Holley	H ₂ O (l)	e ⁻	0.1 - 2 keV	[10]
			ions	0.3 – GeV	
<i>CPA100</i>	Terrissol	H ₂ O (l)	e ⁻	10 eV – 100 keV	[11]
<i>DELTA</i>	Zaider & Brenner	H ₂ O (v,l)	e ⁻	10 eV - 10 keV	[12]
			p & a	0.3 – 4 MeV/u	
<i>ETRACK</i>	Ito	H ₂ O (v)	e ⁻	10 eV - 10 keV	[13]
<i>TRION</i>	Lappa <i>et al</i>	H ₂ O (v,l)	e ⁻	10 eV - 1MeV	[14]
			p & a	0.3 - 4 MeV/u	
<i>KURBUC</i>	Uehara & Nikjoo	H ₂ O (v)	e ⁻	10 eV – 10 MeV	[15]
<i>TRACEL</i>	Tomita <i>et al</i>	H ₂ O (v, l)	e ⁻	10 eV - 1 MeV	[16]
<i>PARTRACK</i>	Paretzke <i>et al</i>	H ₂ O (v, l)	ions	0.3 - GeV	[17]
<i>MOCA14</i>	Wilson & Paretzke	H ₂ O (v)	p & a	0.3 - 4 MeV/u	[18]
<i>PITS</i>	Wilson & Nikjoo	Biological	Ions	0.3 – GeV MeV/u	[19]
<i>LEPHIST</i>	Uehara & Nikjoo	H ₂ O	P	1keV-1MeV	[20]

experimental and theoretical information for constructing cross sections. To start with, the paper provides the current status of the code *kurbuc* as a representative of electron codes and *pits* for simulation of ion track segment. Electron cross sections are described in analytical forms suitable for reproduction by the reader. The paper also describes development of a new model for the description and simulation of tracks for low energy protons from 1keV to 1MeV. Finally, we describe an application of the MCTS for the simulation of the response of proportional counters for light ions.

Charge particle track simulation requires cross sections for elastic, ionization, excitation, partial ionization and excitation, secondary electron spectra. Not all these cross sections are available for materials of biological interest. As water is not a tractable experimental target most data have been obtained in water vapour which imposes a major handicap and hardship on development and verification of the codes. In the past, much discussion has been made on the phase effect. For practical reasons we believe data generated using cross sections obtained in water vapour density corrected for liquid water or DNA are suitable for use in theoretical calculations and modelling in radiation biology.

2. Model basis for electron transport

The code *kurbuc* simulates interaction of electrons 10eV to 10 MeV in water vapour [15]. In the following we summarise the cross sections for ionisations, excitations and elastic scattering adopted

in the code, in an analytical form suitable for numerical reproduction. Elastic scattering cross sections were calculated using Rutherford formula including the Moliere's screening effect. There are some suitable experimental cross sections [21-25] and the NIST [26] library which provides a data set of theoretical cross sections for electron elastic scattering for atoms. Molecular cross sections can then be obtained using additivity rule for a composite molecule such as water. The published experimental and theoretical data were used to obtain a fitted elastic scattering cross section data set for electrons in the range 10 eV to 10 keV for water. A polynomial of the form $\sigma_{\text{ela}} = \sum c_i (\ln T)^{i-1}$ was used to obtain the fitting parameters in two energy ranges. In the energy range $10 \text{ eV} \leq T < 120 \text{ eV}$ ($i=1,6$),

$$\begin{aligned} c_1 &= -667.2442, & c_2 &= 949.4650, \\ c_3 &= -507.5807, & c_4 &= 131.2099, \\ c_5 &= -16.58025, \text{ and} & c_6 &= 0.8234437. \end{aligned}$$

For the energy range $120 \text{ eV} \leq T < 10 \text{ keV}$, $i = 1,4$

$$\begin{aligned} c_1 &= 27.45452, & c_2 &= -9.232332, \\ c_3 &= 1.056612, \text{ and} & c_4 &= -0.04093413. \end{aligned}$$

Experimental excitation cross sections for electrons are a few and mainly taken in water vapour. There are many modes of excitations for energies greater than 10eV. Compilation of data have been made by Paretzke [27], Olivero [28] and Zaider [29]. The code *kurbuc* has adopted the data of Paretzke for the 10 mode of excited states. Total excitation cross sections can be obtained by summing all the individual modes of excitations using the empirical

formula of Berger and Wang [30]. The fitting parameters to the excitation cross section for *kurbuc* is presented as a function of the form $y = p + qx + rx^2 + ax^c [\exp(-bx)]$, where $x = \log(t)$, and

Parameter	<i>Kurbuc</i>
a	0.01608355
b	2.875443
c	11.53760
p	-0.4113672
q	0.1302236
r	-0.008854055

There are various theoretical treatments and experimental data for measurements of the singly differential ionization cross sections for the ejection of an electron generated by collision of an electron with water molecule [19]. Although there is a close agreement among the experimental data over part of the energy spectrum, there is considerable variation in the range 50eV to 1keV. For a general consensus, these data were least square fitted to a function of

the form $\sigma_{\text{exp}} = c + at^r e^{-(b_1t + b_2t^2)}$ where $t = \ln \frac{T}{15}$ in which units of σ is 10^{-16} cm^2 and that of T , the particle kinetic energy, is eV. The fitting parameters are given by

$$a = 2.07201, \quad b_1 = 0.271302, \quad b_2 = 0.119638, \\ r = 1.46521, \quad \text{and} \quad c = 0.074664.$$

3. Model basis for ion transport

Pits is a code for simulation of positive ion track segments in a variety of media for ion energies greater than 0.3 MeV/u. For ion energies below the Bragg peak other processes such as charge exchange needs to be considered as discussed in the next section. The code is organized in a modular form to enable use of different cross sections and link with other track codes for simulation of delta electrons. *PITS* is an implementation of a semi-empirical model developed by Miller et al. [31], for inelastic interactions of charged particles with matter based on the Bethe-Born theory. The theoretical foundation is described in detail in the literature. The most frequent interaction of a fast charged particle with an absorber, is to dislodge valence electrons from their atomic/molecular orbitals, ejecting them frequently with sufficient kinetic energy to travel significant distances through the matter, causing further ionization along their own path. Therefore, the primary information needed for realistic ion-track simulation is the probability for ejecting such electrons (delta-rays). The single differential cross section (SDCS) provides the probability for the energy for an ejected delta-ray. Table III shows a list of experimental dielectric response functions for several media used for evaluating single differential cross sections [27,

32-38]. Figure 1 shows the derived model optical oscillator strengths in various phases for water, carbon and DNA. Output of the code has been tested in terms of stopping power and radial distribution of interactions for various ions. Figure 2 shows comparison of the stopping powers calculated by the code with the ICRU49 [39] data for various ions. Figure 3 shows radial distribution of dose around the core of the particle tracks for ^{16}O and ^{20}Ne ions compared with experimental data of Varma [40, 41] and model calculations by Cucinotta [42].

Table III – References for Dielectric Response Functions of Several Materials.

Material	Ref
Graphite, amorphous	[32]
DNA	[33]
Water, vapour	[27]
Water, liquid	[34-36]
Water, solid-hexagonal	[37]
Water, solid-amorphous	[38]

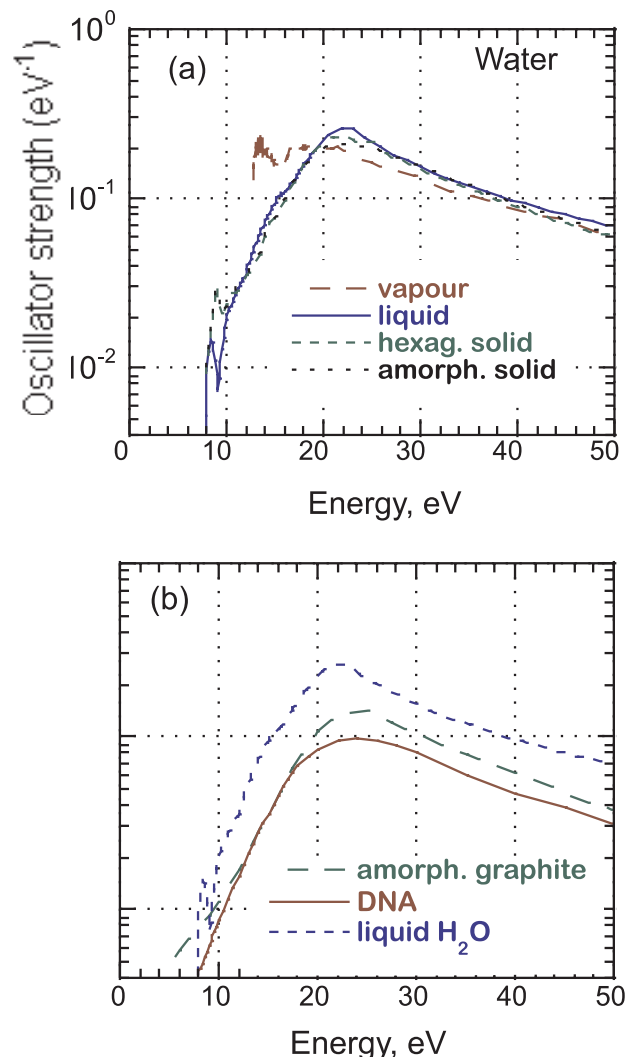


Fig. 1 – Oscillator strength distributions for several media: a) distributions for different water phases and b) for carbon, DNA and liquid water.

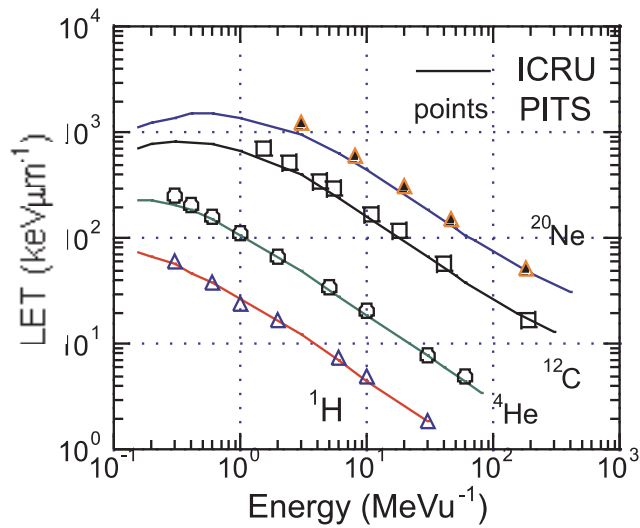
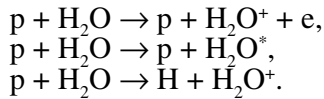


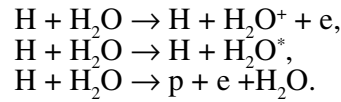
Fig. 2 – Stopping powers calculated from the output of the *pits* code for several ions compared with ICRU data.

4. Low energy protons

Current models of the track structure codes for ions, listed in Table II, generate track segments for ion energies greater than 0.3 MeV/u. At lower energies the energy loss models are not reliable because they lack inclusion of cross sections for many of the important interaction. Accurate treatment of all interactions, including excitation and ionization by dressed ions and neutrals, and charge exchange processes which play an important role in energy degradation of ions at these energies, is needed. The interaction of protons with the stopping medium involves three primary processes



Following electron capture, the moving hydrogen atom can interact with the stopping medium by three primary processes



The calculations for protons and atomic hydrogen stopping in water vapour are based on experimental data as well as the theoretical treatments. The electronic stopping cross section for protons is defined by $L(T) = \sum_j f_p Q_j \sigma_j(T) + \sum_k f_H Q_k \sigma_k(T)$ where j represents interactions leading to ionization, excitation and electron capture by proton impact, and k represents ionization, excitation and electron loss by neutral hydrogen impact; $\sigma(T)$ represents total cross sections for processes k and j at kinetic energy T for proton and atomic hydrogen interactions, respectively; Q is the mean energy transfer in each interaction; and f_p and f_H are the equilibrium charge fractions for protons and atomic hydrogen, respectively.

Total ionization cross sections for protons $\sigma_{ip}(T)$ were determined by the least-square fit to the experimental data given by Rudd et al. [43]. The total electron production cross section for neutral-hydrogen impact were obtained from integrating the double-differential cross section measured by Bolorizadeh and Rudd [44]. The cross section obtained includes contributions from electrons ejected from the target as well as from the projectile by the electron loss process. The latter is known as electron loss to the continuum and was first observed in the electron spectrum in H_2^+ collisions by Wilson and Toburen [45]. The net cross section for ionization of the target water molecule was obtained by su-

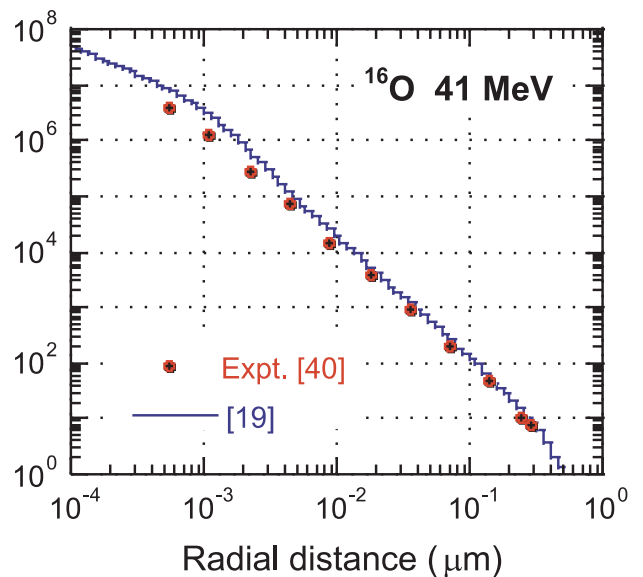
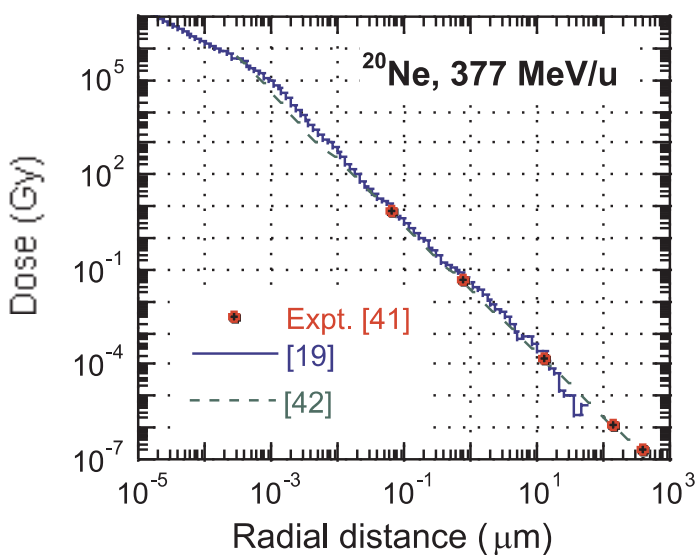


Fig. 3 – Dose distributions around ^{20}Ne (377 MeV/u, 31 keV/ μm) and ^{16}O (41 MeV, 876 keV/ μm) track segments. Data are compared with experimental observations and theoretical calculation.

tracting the electron loss cross section from total ionisation cross sections.

The mean energy transfer for ionization was calculated by summing the average energy of secondary electrons produced by proton impact and the average initial binding energy of the ejected electron. It is assumed that this function is applicable for the proton energies lower than 15 keV where no experimental data is available. For proton energies greater than 100 keV a linear interpolation of the experimental data was used.

Excitation cross sections and mean excitation energy loss by proton and hydrogen impact on water molecules were treated using the formula of Miller and Green [46]. At low ion energies charged particles undergo electron capture and loss events. Total cross sections for electron capture and electron loss for protons and atomic hydrogen were evaluated using the analytical functions given by Miller and Green [46] and fitted to the experimental data of Toburen et al. [47] and Dagnac et al. [48]. Three energy-loss components were taken into account for energy transfer in the electron capture process. These include, energy to remove the electron from the target molecule, the energy to provide translational velocity for the electron to move at the speed of the proton, and energy released from capture into the bound state of the proton. The latter is equal to the binding potential of the state to which the electron is captured. The energy lost by the neutral hydrogen atom in the electron-loss process is simply the binding energy of the projectile electron. The kinetic energy of the electron resulting from the electron-loss process was provided for in the capture process. Figure 4 shows the calculated stopping cross sections and in comparison with the published data [39, 49]. The calculated electronic stopping cross sections are in agreement with the published data within 20% for energies in the range 10keV to 1 MeV. Radial distribution of dose for 1 MeV proton has been compared with experimental and theoretical calculations in Figure 5 [7, 50, 51]

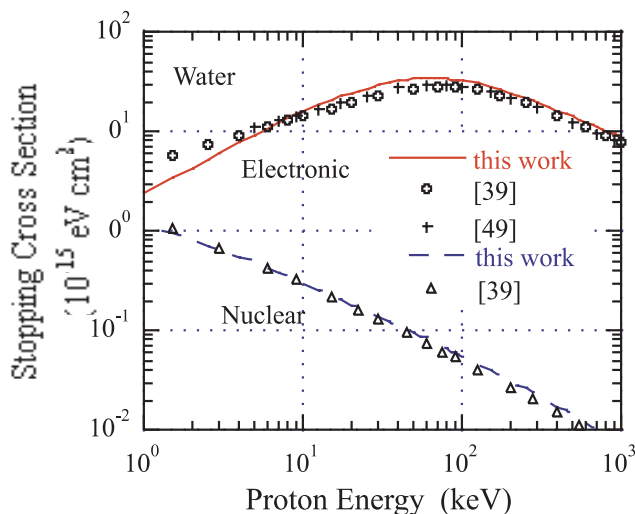


Fig. 4 – Comparison of stopping cross sections as a function of initial energy.

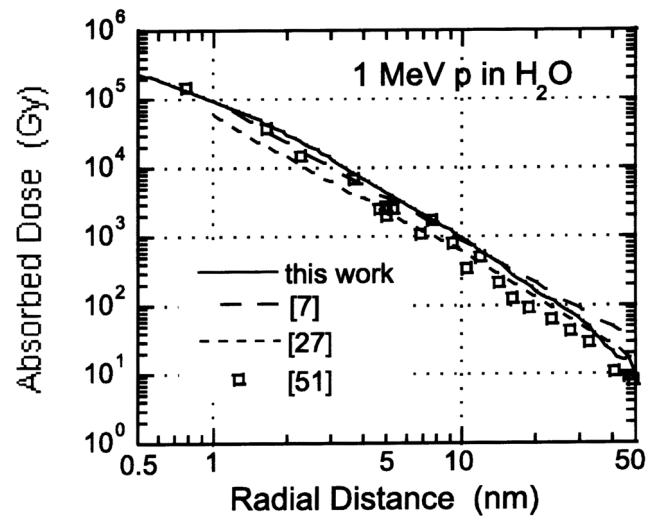


Fig. 5 – Radial dose distribution for 1 MeV protons calculated from the output of the code *lephist*.

5. Model application: the response of a proportional counter

A paper in this volume by Borak et al. describes the response of a tissue-equivalent-proportional-counter (TEPC) to heavy charged particles. In this section we present a preliminary application of track structure to simulate the response of a TEPC counter for 5 MeV alpha-particles. Proportional counters are the main instrument for measurements of microdosimetric parameters. The instrument is either designed as a walled or a wall-less counter. The principle feature of the counter is based on the similarity between the energy loss in the solid wall and the gas cavity as these are made of equivalent density material. Proportional counters are employed in measurement of radiation dose, quality of radiation and spectra of radiation field in the environment under test. It has been used in radiation therapy, microelectronics and radiation biology. Because of its sensitivity, robustness and ease of operation it is used in space on board the satellites and manned space flights for radiation protection purposes.

The simulation of energy absorbed for 5.3 MeV alpha-particles were carried out for a site 1.0 mm diameter sphere. In the walled counter the diameter of gas cavity was set to 6 mm and a gas density of $8.33 \times 10^{-5} \text{ g cm}^{-2}$ similar to the experiment of Gross et al. [52]. Figure 6a shows lineal energy spectrum simulated for 5.3 MeV alpha-particles irradiating a wall-less counter. The distribution of lineal energy as a function of impact parameter is shown in Figure 6b for walled and wall-less counters. Figure 6a shows a non-zero distribution at low event size frequencies which is a deviation from the theoretical chord length distributions. The deviation arise from indirect events entering the sensitive volume of the counter. This is also evident from a small rise in the frequency of events when the impact parameter is nearly the same as the radius of the cavity. The peak

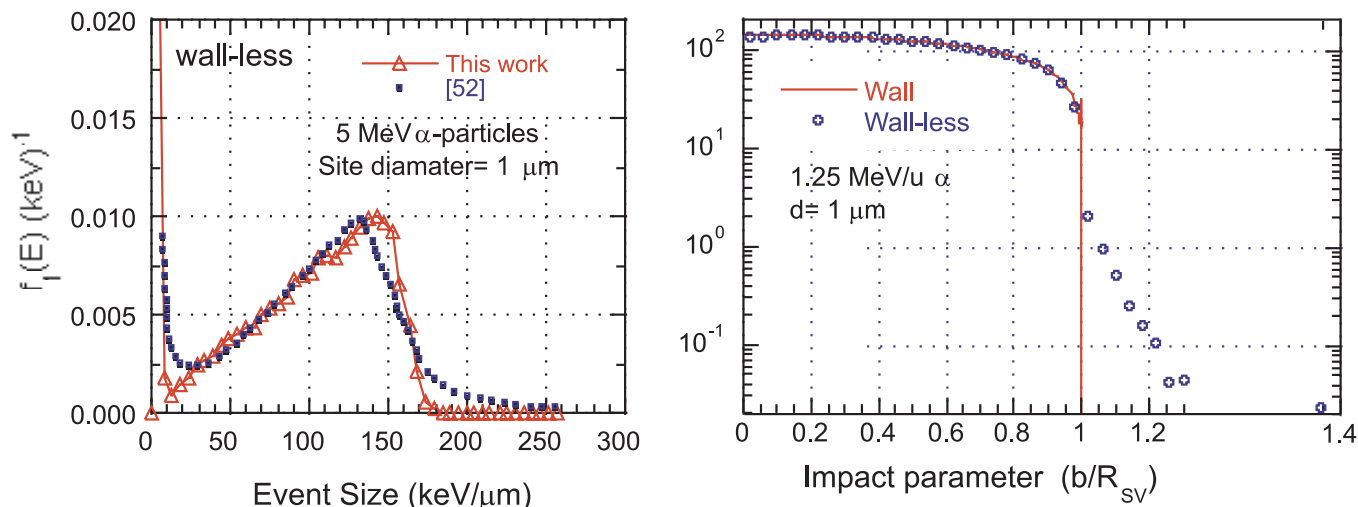


Fig. 6 – The Monte Carlo simulated energy deposition in spherical walled and wall-less TEPC counter for 5 MeV α -particles (94 keV/ μ m).

is small as secondary electrons generated in the wall are not very energetic. The escaping of electrons from cavity is also negligible due to short range of electrons, less than the cavity diameter. However, the contributions from indirect events become prominent with HZE particles [53].

6. Summary

Monte Carlo track structure codes simulate event-by-event interaction of charged particles in medium of interest for biophysical modelling, therapeutic and spectroscopic applications. The input data for electron, ionization, excitation and elastic scattering, cross sections were presented in a form suitable for reproduction. Model output parameters were presented for electron and ion codes. A new model for simulation of full slowing down of low energy protons in the range 1 keV to 1 MeV was presented. Electron and ion tracks generated by the codes *kurbuc* and *pits* were used to simulate the response of a proportional counter to 5 MeV alpha-particles. Data shows the contribution of indirect effect to the response of the counter.

Acknowledgements

The authors would like to thank Steve Thomas for the preparation of the manuscript. The work was partially supported by the European Community programme FIGH-CT-1999-00005.

REFERENCES

- [1] Berger MJ, Seltzer SM. ETRAN, Monte Carlo Code System for electron and photon transport through extended media. ORNL Documentation for RISC Computer code package CCC-107 1973.
- [2] Nelson WR, Hirayama H, Rogers DW. The EGS4 Code System, SLAC-Report-265 1973.
- [3] Berger MJ. Proton Monte Carlo transport programme PTRAN. National Institute of Standards and Technology. Report NISTIR-5113 1993.
- [4] Breitsmeister JF Ed. MCNP - A General Monte Carlo N-Particle transport code. RIST, LA-12625-M Manual 1993.
- [5] Baró J, Sempau J, Fernández-Varea, Salvat, F. PENELOPE: An algorithm for Monte Carlo simulation of the penetration and energy loss of electrons and positrons in matter. Nuclear Instruments and Methods in Physics Research B 1995; 100; 31-46.
- [6] Hartmann Siantar CL, Moses EI. The PEREGRINE™ programme using physics and computer simulation to improve radiation therapy for cancer. European J Phys 1998; 19; 513-521.
- [7] Butts JJ, Katz R. Theory of RBE for heavy ion bombardment of dry enzymes and viruses. Radiat Res 1967; 30; 855-871.
- [8] Paretzke HG. Radiation track structure theory. In: Kinetics of Nonhomogeneous Processes. Freeman GR Ed. New York. John Wiley and Sons 1987; 89-170.
- [9] Turner JE, Magee JL, Wright HA, Chatterjee A, Hamm RN, Ritchie RH. Physical and chemical development of electron tracks in liquid water. Radiat Res 1983; 96; 437-449.
- [10] Chatterjee A, Holley W. Computer simulation of initial events in the biochemical mechanisms of DNA damage. Advances in Radiation Biology 1993; 17; 181-226.
- [11] Terrissol M, Beaudre A. Simulation of space and time evolution of radiolytic species induced by electrons in water. Radiat Prot Dosim 1990; 31; 171-175.
- [12] Zaider M, Brenner DJ, Wilson WE. The applications of track calculations to Radiobiology 1. Monte Carlo simulation of proton tracks. Radiat Res 1983; 95; 231-247.
- [13] Ito A. Calculation of double strand break probability of DNA for low LET radiations based on track structure analysis. Nuclear and Atomic Data for Radiotherapy and Related Radiobiology. International Atomic Energy Agency, IAEA, Vienna 1987.
- [14] Lappa AV, Bigildeev EA, Burmistrov DS, Vasilyev ON. Trion code for radiation action calculations and its application in komicrodosimetry and radiobiology. Radiat Environ Biophys 1993; 32; 1-19.
- [15] Uehara S, Nikjoo H, Goodhead DT. Cross-sections for water vapour for the Monte Carlo electron track structure code from 10 eV to the MeV region. Phys Med Biol 1993; 38; 1841-1858.
- [16] Tomita H, Kai M, Kusama T, Ito A. Monte Carlo

- simulation of physicochemical processes of liquid water radiolysis - The effects of dissolved oxygen and OH scavenger. *Radiation Environmental Biophysics* 1997; 36; 105-116.
- [17] Dingfelder M, Hantke D, Inokuti M, Paretzke HG. Electron inelastic-scattering cross sections in liquid water. *Radiat Phys Chem* 1998; 53; 1-18.
- [18] Wilson WE, Paretzke HG. Calculation of distribution of energy imparted and ionisations by fast protons in nanometer sites. *Radiat Res* 1981; 81; 521-537.
- [19] Wilson WE, Nikjoo H, 1999. A Monte Carlo code for Positive Ions Track Simulation. *Radiat Environm Biophys* 2000; 38; 97-104.
- [20] Uehara S, Nikjoo H. *LEPHIST*, a Monte Carlo track structure code for low energy protons (in preparation).
- [21] Shyn TW, Cho SY. Vibrationally elastic scattering cross section of water vapor by electron impact. *Phys Rev* 1987; A36; 5138-5142.
- [22] Hayashi M. Electron collision cross-sections for atoms and molecules determined from beam and swarm data. IAEA-TECDOC-506 1989; 194-200.
- [23] Katase A, Ishibashi K, Matsumoto Y, Sakae T, Maezono S, Murakami E, Watanabe K, Maki H. Elastic scattering of electrons by water molecules over the range 100-1000 eV. *J Phys* 1986; B19; 2715-2734.
- [24] Nishimura H. Elastic scattering cross-sections of H₂O by low energy electrons. In: *Electronic and Atomic Collisions*. Proc. XIth Int. Conf. Oda N, Takayanagi K Eds. Amsterdam. North-Holland 1979; 314.
- [25] Danjo A, Nishimura H. Elastic scattering of electrons from H₂O molecule. *J Phys Soc Jpn* 1985; 54; 1224-1227.
- [26] NIST standard reference database #64. Elastic-Electron-Scattering Cross-Section Database. Gaithersburg. US Dept of Commerce 1996.
- [27] Paretzke HG, Simulation von Elektronenspuren in Energiebereich 0.01-10 keV. In: *GSF-Bericht. Gesellschaft für Strahlen-und Umwelt Forschung. Munchen. Wasserdampf* 1988; 24-88.
- [28] Olivero JJ, Stagat RW, Green AES. Electron deposition in water vapour, with atmospheric applications. *J Geophys Res* 1972; 77; 4797-4811.
- [29] Zaider M, Brenner DJ, Wilson WE. The applications of track calculations to radiobiology, I. Monte Carlo simulation of proton tracks. *Radiat Res* 1983; 95; 231-247.
- [30] Berger M, Wang R. Multiple scattering angular deflections and energy-loss straggling. Monte Carlo transport of Electrons and Photons. Jenkins TM, Nelson WR, Rindi A Eds. New York. Plenum 1988; 21-56.
- [31] Miller JH, Wilson WE, Manson ST. Secondary electron spectra: A semiempirical model. *Radiat Prot Dosim* 1985; 13; 27-30.
- [32] Arakawa ET, Dolfini SM, Ashley JC, Williams MW. Arc-evaporated carbon films: optical properties and electron mean free paths. *Phys Rev B* 1985; 31; 8097-8101.
- [33] Inagaki T, Hamm RN, Arakawa ET, Painter LR. Optical and ielectric properties of DNA in the extreme ultraviolet. *J Chem Phys* 1974; 61; 4246-4250.
- [34] Heller JM Jr, Hamm RN, Birkhoff RD, Painter LR. Collective oscillation in liquid water. *J Chem Phys* 1974; 60; 3483-3486.
- [35] Hayashi H, Watanabe N, Udagawa Y. Optical spectra of liquid water in vacuum uv region by means of inelastic X-ray scattering spectroscopy. *J Chem Phys* 1998; 108; 823-825.
- [36] Watanabe N, Hayashi H, Udagawa Y. Bethe surface of liquid water determined by inelastic scattering spectroscopy and electron correlation effect. *Bull Chem Soc Jpn* 1997; 70; 719-726.
- [37] Seki M, Kobayashi K, Nakahara J. Optical spectra of hexagonal ice. *J Phys Soc Jpn* 1981; 50; 2643-2648.
- [38] Kobayashi K. Optical spectra and electronic structure of ice. *J Phys Chem* 1983; 87; 4317-4321.
- [39] ICRU Report 49. International Commission of Radiation Units and Measurements. Bethesda, MD 1993.
- [40] Varma MN, Paretzke HG, Baum JW, Lyman JT, Howard J. Dose as a function of radial distance from a 930 MeV 4He ion beam. In: *Proceedings 5th Symposium on Microdosimetry*. 1975; 75-95.
- [41] Varma MN, Baum JW, Kuchner AV. Radial dose, LET and W for 16O ions in N₂ and tissue-equivalent-gases. *Radiat Res* 1977; 70; 511-518.
- [42] Cucinotta FA, Katz R, Wilson JW. Radial distribution of electron spectra from high-energy ions. *Radiat Environ Biophys* 1998; 37; 259-265.
- [43] Rudd ME, Goffe TV, DuBois RD, Toburen LH. Cross sections for ionization of water vapor by 7-4000-keV protons. *Phys Rev* 1985; A31; 492-494.
- [44] Bolorizadeh MA, Rudd ME. Angular and energy dependence of cross sections for ejection of electrons from water vapour. I. 50-2000 eV electron impact. *Phys Rev* 1986; A33; 882-887.
- [45] Wilson WE, Toburen LH. Electron emission in H₂⁺ - H₂ collisions from 0.6 to 1.5 MeV. *Phys Rev* 1973; A7; 1535-1543.
- [46] Miller JH, Green AES. Proton energy degradation in water vapor. *Radiat Res* 1973; 54; 343-363.
- [47] Toburen LH, Nakai MY, Langley RA. Measurement of high-energy charge-transfer cross sections for incident protons and atomic hydrogen in various gases. *Phys Rev* 1968; 171; 114-122.
- [48] Dagnac R, Blanc D, Molina D. A study on the collision of hydrogen ions H₁⁺, H₂⁺ and H₃⁺ with a water-vapour target. *J Phys* 1970; B3; 1239-1251.
- [49] Janni JF. *Atomic Data and Nuclear Data Tables* 27, no. 2-5. 1982.
- [50] Wingate CL, Baum JW. Measured distributions of dose and LET for alpha and proton beams in hydrogen and tissue-equivalent gas. *Radiat Res* 1976; 65; 1-19.
- [51] Paretzke HG, Eickel R, Waker A. Comparison of track structure calculations with experimental results. In: *Microdosimetry, fourth symposium, Pallanza (Italy)*, Euratom 1973. EUR5122 d-e-f; 141-165.
- [52] Gross W, Biavati BJ, Rossi HH. Microdosimetry of directly ionizing particles with wall-less proportional counters. In: *Microdosimetry, second symposium, Stresa (Italy)*, Euratom 1969. EUR 4452 d-e-f; 249-261.
- [53] Rademacher SE, Borak TB, Zeitlin C, Heilbronn L, Miller J. Wall effects observed in tissue-equivalent proportional counters from 1.05 GeV/nucleon iron-56 particles. *Radiat Res* 1998; 149; 387-395.